

# Development of a Point Location Conversion Approach for Distance Cartogram Construction

TAKESHI MIURA<sup>1,a)</sup> KATSUBUMI TAJIMA<sup>1</sup>

Received: April 16, 2019, Accepted: September 11, 2019

**Abstract:** Distance cartograms are deformed maps in which the distance of each of the preselected point pairs in the geographic map is changed in step with a specified value. In distance cartogram construction, the preselected points such as train stations are fixed in the first step, and other points such as those comprising railroads are fixed in the second step. This paper proposes a new point location conversion approach for the second step. In the approach, a triangle in the geographic map which consists of two points already fixed in the first step and a point to be fixed in the second step, is converted into a similar triangle in the cartogram. The experimental results demonstrate its effectiveness.

**Keywords:** map deformation, cartogram, distance cartogram, homeomorphism

## 1. Introduction

Nowadays, a large number of geographically-referenced statistical datasets are available. Visualizing information on the above type of dataset is considered effective for intuitively comprehending it overall and using the map deformation technique or namely constructing a cartogram is an effective approach for visualization [1], [2]. In particular, distance cartograms, in which the distance of each of the preselected point pairs is changed in step with the corresponding specified value are often used as time-space maps where the above distance is replaced by a travel time [3], [4].

The construction process of a distance cartogram generally consists of two steps [3], [4]. The locations of the points included in the preselected pairs such as those corresponding to train stations and bus stops are fixed in the first step whereas the locations of other points such as those comprising railroads and boundaries between municipalities are fixed in the second step. Several effective approaches have been proposed for the first step [3], [4], [5]. Here, we focus on the second step. To maintain the readability of the obtained cartogram, the homeomorphism [3], [4] and the geometrical characteristics of the original geographic shapes, e.g., continuity and differentiability of a line or a curve, must be maintained in this step. However, these conditions are not necessarily satisfied in the approaches previously proposed as will be shown in Section 3.

To improve the property of maintaining the above conditions, we propose a new point location conversion approach used in the second step. In the approach, we aim at maintaining the local configuration of a set of selected points. Specifically, we convert a triangle in the geographic map, which consists of a pair of two points already fixed in the first step and an input point to

be fixed in the second step, into the corresponding triangle in the cartogram, maintaining the similarity of the two triangles. Multiple point-location candidates for a single input point, obtained from a set of multiple triangles including the same input point, are statistically summarized and finally fixed at a single position.

We conducted experiments in which simple artificial mapping models and an actual geographic dataset were used. We compared the proposed approach with the other two approaches previously proposed. The experimental results showed that the proposed approach could provide better characteristics than those of the other approaches.

## 2. Point Location Conversion Algorithm

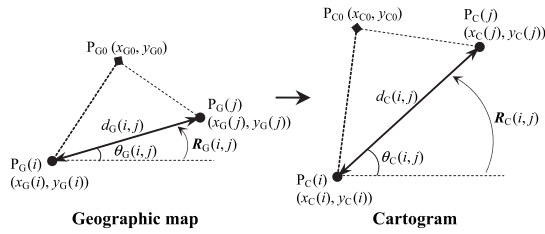
This section describes details of the point location conversion approach. Consider the case that the set of the points in the geographic map,  $P_G(i)(x_G(i), y_G(i))$ <sup>\*1</sup> for  $1 \leq i \leq N$  ( $N$ : total number of points), was already converted into the set of the corresponding points in the cartogram,  $P_C(i)(x_C(i), y_C(i))$  for  $1 \leq i \leq N$ , in the first step of cartogram construction process. In the second step, we give the point  $P_{G0}(x_{G0}, y_{G0})$  in the geographic map as an input to be converted into the output point  $P_{C0}(x_{C0}, y_{C0})$  in the cartogram as shown in **Fig. 1**. We assume that the angles between the horizontal axis and the directions of the pair of the  $i$ th and  $j$ th points,  $\overrightarrow{P_G(i)P_G(j)}$  and  $\overrightarrow{P_C(i)P_C(j)}$ , are given as  $\theta_G(i, j)$  and  $\theta_C(i, j)$ , respectively. The rotation from the horizontal axis to  $\overrightarrow{P_G(i)P_G(j)}$  and that to  $\overrightarrow{P_C(i)P_C(j)}$  are respectively represented by the following rotation matrices:

$$R_G(i, j) = \begin{bmatrix} \cos \theta_G(i, j) & -\sin \theta_G(i, j) \\ \sin \theta_G(i, j) & \cos \theta_G(i, j) \end{bmatrix} \quad (1)$$

<sup>\*1</sup> In this paper, the symbol  $x$  is used as the coordinate of the horizontal axis, whereas  $y$  as that of the vertical axis. This symbol assignment is contrary to that in the Japanese surveying and mapping community ( $x$ : northing,  $y$ : easting) [6]. We select the above assignment in accordance with mathematical conventions.

<sup>1</sup> Graduate School of Engineering Science, Akita University, Akita 010-8502, Japan

<sup>a)</sup> miura@mail.ee.akita-u.ac.jp



When  $\Delta P_{G0}P_G(i)P_G(j)$  and  $\Delta P_{C0}P_C(i)P_C(j)$  are similar to each other:

$$\begin{aligned}
 \mathbf{p}_{C0} &= \mathbf{R}_{CG}(i,j) \{ \mathbf{p}_{G0} - \mathbf{p}_G(i) \} + \mathbf{p}_C(i) \\
 (\mathbf{p}_{G0} &= [x_{G0} \ y_{G0}]^T, \ \mathbf{p}_G(i) = [x_G(i) \ y_G(i)]^T, \\
 \mathbf{p}_{C0} &= [x_{C0} \ y_{C0}]^T, \ \mathbf{p}_C(i) = [x_C(i) \ y_C(i)]^T, \\
 \mathbf{R}_{CG}(i,j) &= \frac{d_C(i,j)}{d_G(i,j)} \mathbf{R}'_{CG}(i,j) = \frac{d_C(i,j)}{d_G(i,j)} \mathbf{R}_C(i,j) \mathbf{R}_G(i,j)^{-1}
 \end{aligned}$$

Fig. 1 Concept of point location conversion.

$$\mathbf{R}_C(i,j) = \begin{bmatrix} \cos \theta_C(i,j) & -\sin \theta_C(i,j) \\ \sin \theta_C(i,j) & \cos \theta_C(i,j) \end{bmatrix} \quad (2)$$

The above matrices satisfy  $\mathbf{R}_C(i,j) = \mathbf{R}'_{CG}(i,j) \mathbf{R}_G(i,j)$  where  $\mathbf{R}'_{CG}(i,j)$  is the rotation matrix from  $\overrightarrow{P_G(i)P_G(j)}$  to  $\overrightarrow{P_C(i)P_C(j)}$ , and consequently  $\mathbf{R}'_{CG}(i,j) = \mathbf{R}_C(i,j) \mathbf{R}_G(i,j)^{-1}$  is given. By assuming that  $\Delta P_{G0}P_G(i)P_G(j)$  and  $\Delta P_{C0}P_C(i)P_C(j)$  are similar to each other, we can fix the location of  $P_{C0}$  as follows:

$$\mathbf{p}_{C0} = \mathbf{R}_{CG}(i,j) \{ \mathbf{p}_{G0} - \mathbf{p}_G(i) \} + \mathbf{p}_C(i) \quad (3)$$

where

$$\begin{aligned}
 \mathbf{p}_{G0} &= [x_{G0} \ y_{G0}]^T, \ \mathbf{p}_G(i) = [x_G(i) \ y_G(i)]^T, \\
 \mathbf{p}_{C0} &= [x_{C0} \ y_{C0}]^T, \ \mathbf{p}_C(i) = [x_C(i) \ y_C(i)]^T, \\
 \mathbf{R}_{CG}(i,j) &= \frac{d_C(i,j)}{d_G(i,j)} \mathbf{R}'_{CG}(i,j) = \frac{d_C(i,j)}{d_G(i,j)} \mathbf{R}_C(i,j) \mathbf{R}_G(i,j)^{-1} \\
 &= \frac{d_C(i,j)}{d_G(i,j)} \begin{bmatrix} r_{11}(i,j) & r_{12}(i,j) \\ r_{21}(i,j) & r_{22}(i,j) \end{bmatrix}, \\
 d_G(i,j) &= |\mathbf{p}_G(j) - \mathbf{p}_G(i)|, \ d_C(i,j) = |\mathbf{p}_C(j) - \mathbf{p}_C(i)|, \\
 r_{11}(i,j) &= \cos \theta_C(i,j) \cos \theta_G(i,j) + \sin \theta_C(i,j) \sin \theta_G(i,j), \\
 r_{12}(i,j) &= \cos \theta_C(i,j) \sin \theta_G(i,j) - \sin \theta_C(i,j) \cos \theta_G(i,j), \\
 r_{21}(i,j) &= \sin \theta_C(i,j) \cos \theta_G(i,j) - \cos \theta_C(i,j) \sin \theta_G(i,j), \\
 r_{22}(i,j) &= \sin \theta_C(i,j) \sin \theta_G(i,j) + \cos \theta_C(i,j) \cos \theta_G(i,j)
 \end{aligned}$$

and the vector  $\mathbf{p}_{C0}$  corresponds to the location of  $P_{C0}$ . In general, the point configuration in the cartogram is different from the original point configuration in the geographic map. Therefore, Eq. (3) is not necessarily satisfied at every point pair.

Taking the above situation into account, we fix the location of  $P_{C0}$ , i.e., determine the coordinate values of  $\mathbf{p}_{C0}$ , using the weighted mean of location candidates obtained from a set of selected point pairs as follows:

$$\mathbf{p}_{C0} = \frac{\sum_{i,j \in T} w(i,j) \{ \mathbf{R}_{CG}(i,j) \{ \mathbf{p}_{G0} - \mathbf{p}_G(i) \} + \mathbf{p}_C(i) \}}{\sum_{i,j \in T} w(i,j)} \quad (4)$$

$$w(i,j) = \frac{1}{\{d_0(i)d_0(j)\}^q}, \quad d_0(i) = |\mathbf{p}_{C0} - \mathbf{p}_C(i)|$$

where  $w(i,j)$  is the weight assigned to the pair of the  $i$ th and  $j$ th points,  $d_0(i)$  is the distance between  $P_{C0}$  and  $P_C(i)$ ,  $q$  is the parameter to adjust the strength of the weight (actual value: set by

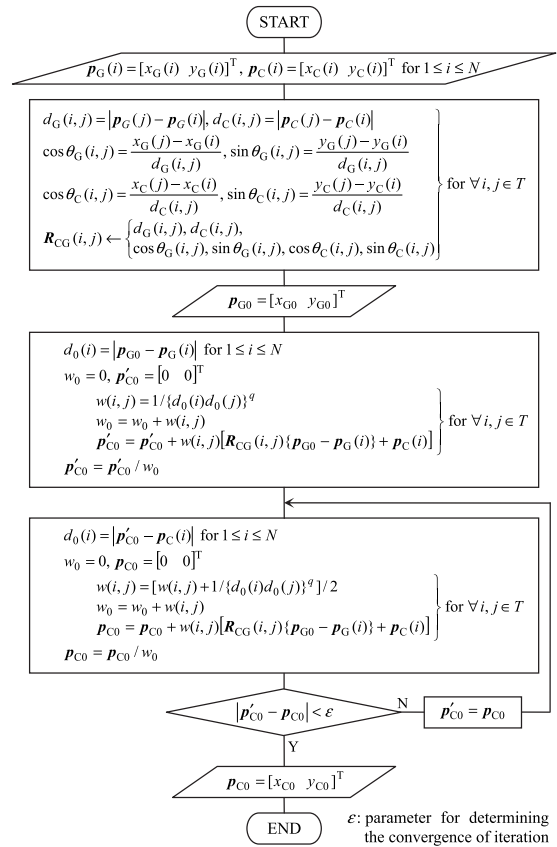


Fig. 2 Point location conversion algorithm.

users) and  $T$  is the set of all the selected point pairs. This weight assignment gives the characteristic that the closer the point  $P_{C0}$  is to any of the points  $P_C(i)$  and  $P_C(j)$ , the more the  $i$ - $j$  point pair is weighted. The above weight includes information on the vector  $\mathbf{p}_{C0}$ . However, the true coordinate values of  $\mathbf{p}_{C0}$  cannot be obtained unless the location of  $P_{C0}$  is fixed. Therefore, we adopt an algorithm shown in Fig. 2 in which the weight values are iteratively calculated with the renewal of  $\mathbf{p}_{C0}$  (the initial  $d_0(i)$  values are replaced by those in the geographic map). As for the setup of  $T$  on the other hand, we use the sum of the following two sets: the set of the point pairs each of which corresponds to both ends of the edge extracted by the Delaunay triangulation [7] of the point configuration in the geographic map, and that extracted from the cartogram. The computational complexity of the proposed algorithm is  $O(N \log N)^{*2}$  (This is the same as the case that the combination of triangulation and barycentric interpolation is used as a point location conversion approach [4]).

### 3. Results

This section presents the experimental results of the proposed approach. First, simple artificial mapping models are used to compare the performance of the proposed approach with those of the following two approaches previously proposed: the moving-least-squares based affine deformation [3] and the combination of the Delaunay triangulation and barycentric interpolation [4].

\*2 The Delaunay triangulation for the setup of  $T$  takes  $O(N \log N)$  [7], whereas the calculation of the weighted mean takes  $O(N)$  because the number of triangulation edges is at most  $3N - 6$  [7]. Therefore, the complexity of the overall algorithm becomes  $O(N \log N)$ .

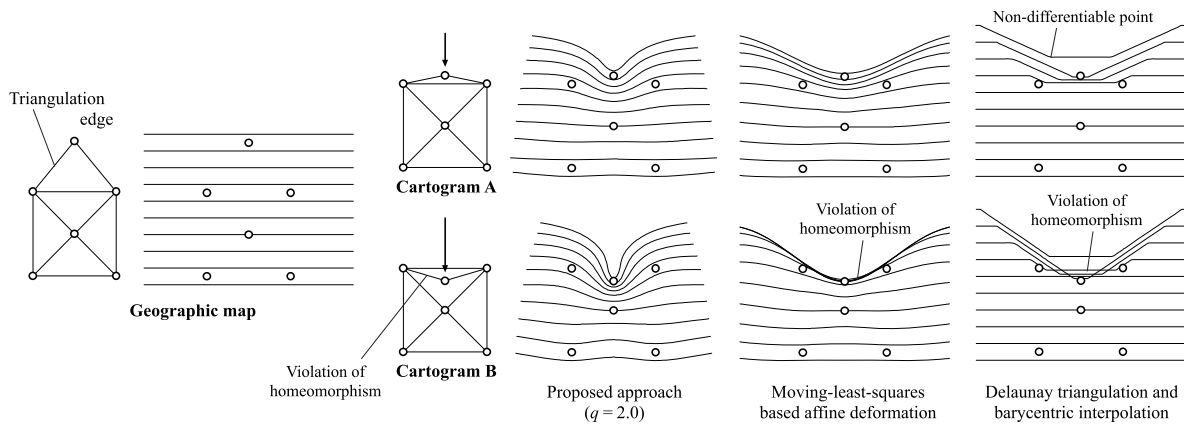


Fig. 3 Cartogram construction for simple artificial mapping models.

Next, the map of the six prefectures of the northeastern area of Japan is used to evaluate the characteristics of the proposed approach.

Figure 3 shows the results of the artificial mapping models. The geographic map consists of 6 points and 10 regular-interval parallel lines, and is converted into the following two cartograms: Cartograms A and B. The locations of the 6 points in the cartograms are fixed in advance (i.e., regarded as already fixed in the first step of cartogram construction process), and the 10 lines are then converted into those in each cartogram by the proposed approach or the other two approaches. In both Cartograms A and B the point located at the highest position in the geographic map is moved downward. That point is still highest in A, whereas it is moved to a position lower than the other two points in B. In other words, Cartogram B is more highly deformed than Cartogram A. This can be confirmed by the homeomorphism of the triangulation edges of the geographic map as shown in Fig. 3 (A: no violation, B: violated).

In the case that the present approach is used (we set  $q = 2.0$  for Eq. (4) and  $\varepsilon = (\text{mean point-pair distance in the converted point configuration}) \times 10^{-3}$  for the iteration process in Fig. 2), both the results of A and B show no violation of homeomorphism in the converted configuration. Moreover, all the lines are smoothly deformed without the appearance of non-differentiable point that does not exist in the lines of the geographic map. On the other hand, in the case that the moving-least-squares approach is used, no non-differentiable point is seen in either A or B. However, a violation of homeomorphism is seen in B. As for the case that the Delaunay-triangulation barycentric-interpolation approach is used, many non-differentiable points are seen in both A and B. In addition, the violation of homeomorphism is also seen in B. The above results suggest that the proposed approach is more robust against a highly deformed point-configuration conversion than the other two approaches.

Figure 4 shows the mapping results for the six prefectures of the northeastern area of Japan. In this case, the configuration of 17 points in the geographic map (upper left of Fig. 4) is converted into that in the cartogram in advance (i.e., in the first step of cartogram construction process), based on the travel times of

the preselected 26 point pairs (upper center of Fig. 4<sup>\*3</sup>). The resulting configuration is shown in the upper right of Fig. 4. This was obtained by applying the distance cartogram construction algorithm of Ref. [5] to the point configuration shown in the upper center of Fig. 4<sup>\*4</sup>. After the above conversion, the proposed approach is used to convert the railroad network and the boundaries between prefectures (Their original configuration is shown at the upper left in Fig. 4) into those in the cartogram.

The obtained cartograms are shown at the bottom of Fig. 4. Three cartograms differing in the value of the parameter  $q$  are shown (However,  $\varepsilon$  in all the cartograms is identical to the case of Fig. 3). The homeomorphism is not violated in any of the obtained cartograms. On the other hand, the shapes of the three cartograms are respectively different, even though the same point configuration is used. This means that users can adjust the shape of a cartogram to a certain extent by varying the  $q$  value.

The calculation times of the  $q = 1.5, 2.0$  and  $3.0$  cases are 281, 281 and 328 ms, respectively (CPU: Intel Core i3-350M). From the above values, we can estimate that the calculation time falls within a range of a few dozen seconds even when the data size is about 100 times that of the present case because the computational complexity of the proposed algorithm is  $O(N \log N)$  as already mentioned. This is short enough to allow users to perform interactive trial-and-error processing for the  $q$ -value adjustment to obtain a cartogram with a more preferable shape.

#### 4. Conclusion

The main contribution of this paper is to provide a distance cartogram construction approach to appropriately convert the location of a point in a geographic map into that in a cartogram. The experimental results show the robustness of the proposed approach against a highly deformed configuration in a cartogram. This report also suggests the adjustability of the proposed approach to obtain a cartogram with a more preferable shape. To clarify the applicability to datasets other than travel times, e.g., a

<sup>\*3</sup> The travel-time dataset of this figure is quoted from Fig. 5 of Ref. [8]. This dataset was organized based on the time-table data of Japan Railways, private railways and bus routes in Yamagata Prefecture and four neighboring prefectures for 1996 [8].

<sup>\*4</sup> In the configuration conversion of the preselected 17 points, several point links (gray lines in Fig. 4) were weighted with a small value (i.e., 0.1) to improve the readability of the deformed configuration.

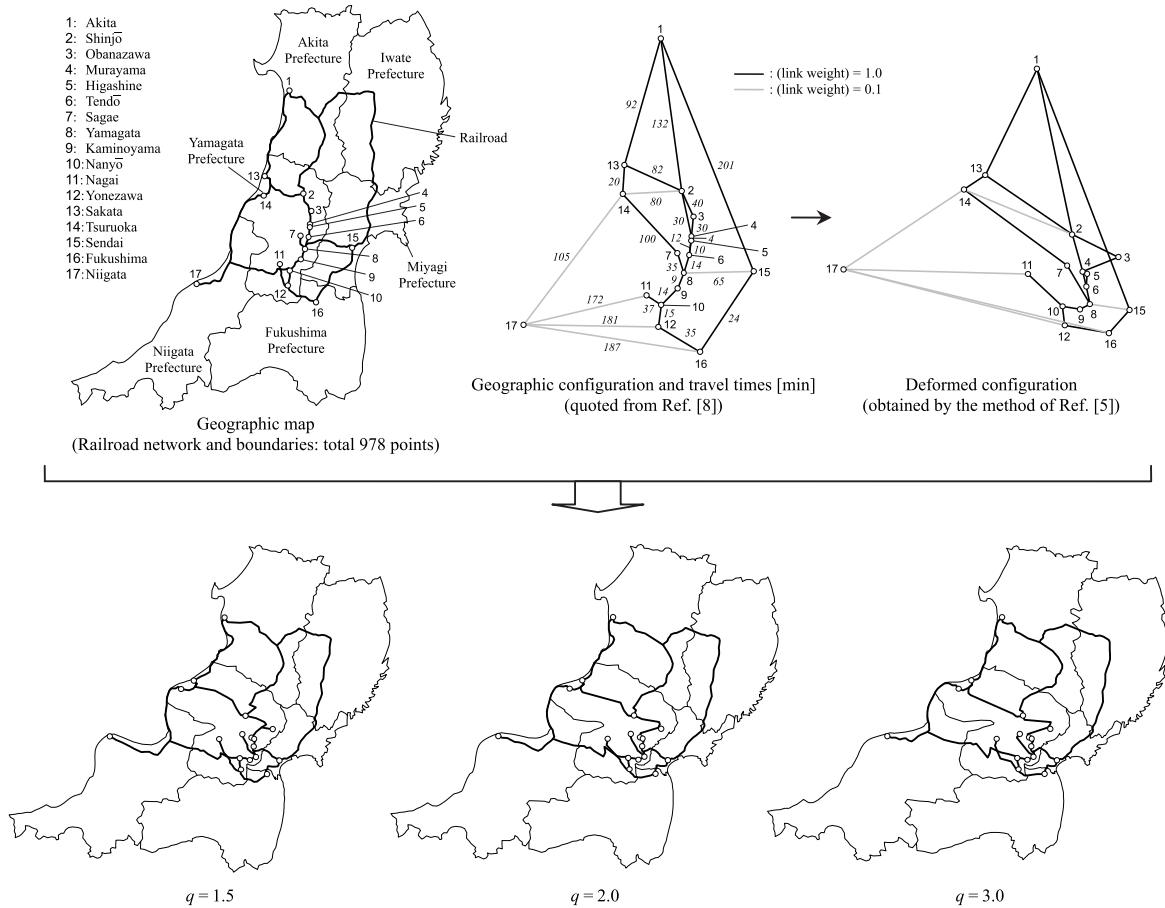


Fig. 4 Cartogram construction for the six prefectures of the northeastern area of Japan.

geographically-referenced dataset related to humanities, will be the subject of future work.

**Acknowledgments** This study was supported by JSPS Grants-in-Aid for Scientific Research (KAKENHI) Grant Number JP18K11981.

**References**

[1] Nusrat, S. and Kobourov, S.: The State of the Art in Cartograms, *EuroVis 2016 Proc. Eurographics/IEEE VGTC Conf. Visualization*, pp.619–642 (2016).

[2] Markowska, A. and Korycka-Skorupa, J.: An Evaluation of GIS tools for Generating Area Cartograms, *Polish Cartographical Review*, Vol.47, No.1, pp.19–29 (2015).

[3] Ullah, R. and Kraak, M.-J.: An Alternative Method to Constructing Time Cartograms for the Visual Representation of Scheduled Movement Data, *Journal of Maps*, Vol.11, No.4, pp.674–687 (2015).

[4] Bies, S. and van Kreveld, M.: Time-Space Maps from Triangulations, Didimo, W. and Patrignani, M. (Eds.), *GD 2012, LNCS 7704*, pp.511–516 (2013).

[5] Shimizu, E. and Inoue, R.: A New Algorithm for Distance Cartogram Construction, *International Journal of Geographical Information Science*, Vol.23, No.11, pp.1453–1470 (2009).

[6] Okazawa, H., Kubodera, T., Sasada, K., Tasumi, M., Hosokawa, Y., Matsuo, E. and Mihara, M.: *Newer Surveying —Fundamentals and Applications with Newest Technology*, Corona Publishing Co., Ltd. (2014) (in Japanese).

[7] Kang, I.-S., Kim T.-W. and Li, K.-J.: A Spatial Data Mining Method by Delaunay Triangulation, *Proc. 5th ACM Workshop on Geographic Information Systems (GIS 97)*, pp.35–39 (1997).

[8] Kotoh, H.: Visualization of Time-Distance Network and Analysis of Regional Structures —The Multi-City Structure of Tohoku Region, *Annual Review of Tohoku University of Art and Design*, No.3, pp.94–103 (1996) (in Japanese).



**Takeshi Miura** received his D.Eng. degree in electrical engineering from Hokkaido University in 1998. He is currently an associate professor in the Department of Mathematical Science and Electrical-Electronic-Computer Engineering, Graduate School of Engineering Science, Akita University.



**Katsubumi Tajima** received his D.Eng. degree in electrical engineering from Tohoku University in 1998. He is a professor in the Cooperative Major in Life Cycle Design Engineering, Graduate School of Engineering Science, Akita University.